energies

MDPI

Article

Comparison of Advanced Charge Strategies for Modular Cascaded Battery Chargers

Nicolas T. D. Fernandes [1,*], Anderson Rocha [2], Danilo Brandao [1] and Braz C. Filho [1]

[1] Graduate Program in Electrical Engineering, Universidade Federal de Minas Gerais, Belo Horizonte 31270-901, Brazil; dibrandao@ufmg.br (D.B.); braz.cardoso@ieee.org.br (B.C.F.)
[2] Centro Federal de Educação Tecnológica de Minas Gerais-CEFET-MG, Belo Horizonte 30421-169, Brazil; andersonrocha@cefetmg.br
* Correspondence: nicolastdf@ufmg.br

Abstract: Although the literature extensively covers the development of battery chargers control strategies, a comparison of these strategies remains a literary gap. The inherent conditions (i.e., State of Health and State of Charge) of each unit in the Battery Energy Storage Systems directly influence the charger control techniques for extending battery lifetime, which makes modular battery chargers an appealing topology for this analysis. This work groups charger control strategies presented in the literature into two: Adapted SoC strategies, directly linked to the field of overstress management, and SoH strategies, which are directly linked to the field of wear-out management. The methodology for comparing the control strategies encompasses battery lifetime, charger, and photovoltaic plant models. Three distinct cases were simulated using real measure data from a solar power plant and a battery model provided by MathWorks®. The results evidence that the Capacity Fade and Energy Throughput strongly depend on the strategy. The controller action evidences the previous statement, as the strategies have different goals that are related to each field. Furthermore, this work analyses the effect of the estimation process in the action of the controller.

Keywords: Battery Energy Storage System; battery charger; ion-lithium battery; energy time-shift PV

Citation: Fernandes, N.T.D.; Rocha, A.; Brandao, D.; Filho, B.C. Comparison of Advanced Charge Strategies for Modular Cascaded Battery Chargers. *Energies* **2021**, *14*, 3361. https://doi.org/10.3390/en14123361

Academic Editor: Woojin Choi

Received: 31 March 2021
Accepted: 10 May 2021
Published: 8 June 2021

1. Introduction

Transiting to a non-fossil energy matrix is essential to mitigate the effects that are related to global warming [1]. The main efforts to reduce CO_2 emissions are related to the introduction of renewable intermittent energy sources and the expansion of the electrification of energy systems. Energy Storage Systems play a major role in enabling renewable energy systems, as they balance and smooth variations in both load and generation [2]. Furthermore, energy storage is key in reducing the costs of renewable energy grids operating with intermittent energy sources. Among different options of energy storage, batteries have important advantages, such as high technological maturity, modularity, facilitated adaptability, and relatively low maintenance in up-to-date energy systems. Another energy storage option that is gaining prominence is fuel-cells, but these devices present technical challenges, such as those described in [3].

The Battery Energy Storage Systems (BESS) consists of battery banks, power-conditioning systems (PCS), control techniques, and the balance of the plant (BoP) [4]. Studies that are related to batteries, PCS, and control are receiving major attention due to the growing importance of energy storage worldwide. Significant scientific efforts on developing control techniques of battery chargers aim at improving charger efficiency and, thus, prolonging the battery lifespan [5–9]. Examples of the addressed problems in the field comprise charging strategies [5], optimization, balancing and integration of modular chargers [6–8], and charge estimation methods [9]. These techniques depend on the active control of each element of interest, which can vary from modules to cells. In this sense, modular chargers are becoming increasingly relevant and achieving greater interest in the scientific community.

Modular chargers can be classified into two main categories: Modular Cascaded Chargers (MCC), in which each module comprises a DC-DC converter with a battery unit (Figure 1) [10], or Modular Multilevel Chargers (MMC), in which each module comprises a DC-AC converter (Figure 2) [11]. In Figure 1, three converters are connected through a Power Conditioning System (PCS), which interfaces the BESS with the electrical grid network. Figure 2 shows four converters in a single-phase MMC application; note that the PCS is missing, which means that the action of the PCS must be performed by the converters that are connected to the battery. This paper focuses on the MCC charger.

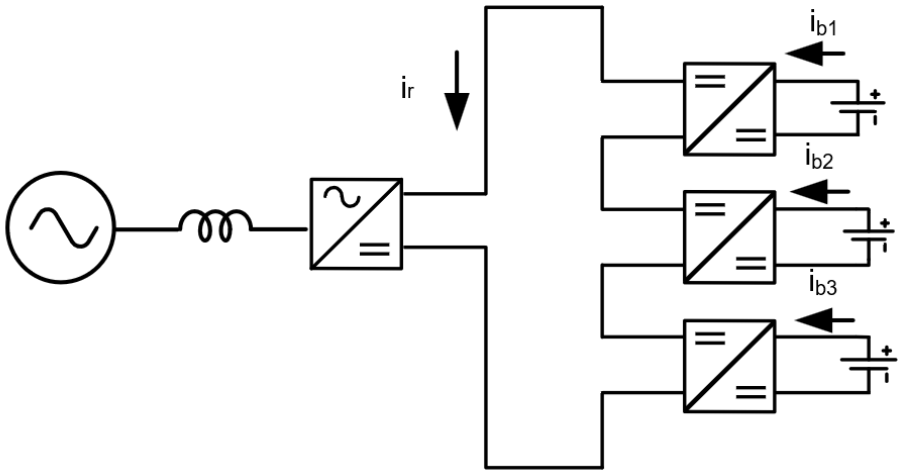

Figure 1. Modular Cascaded Charger (MCC).

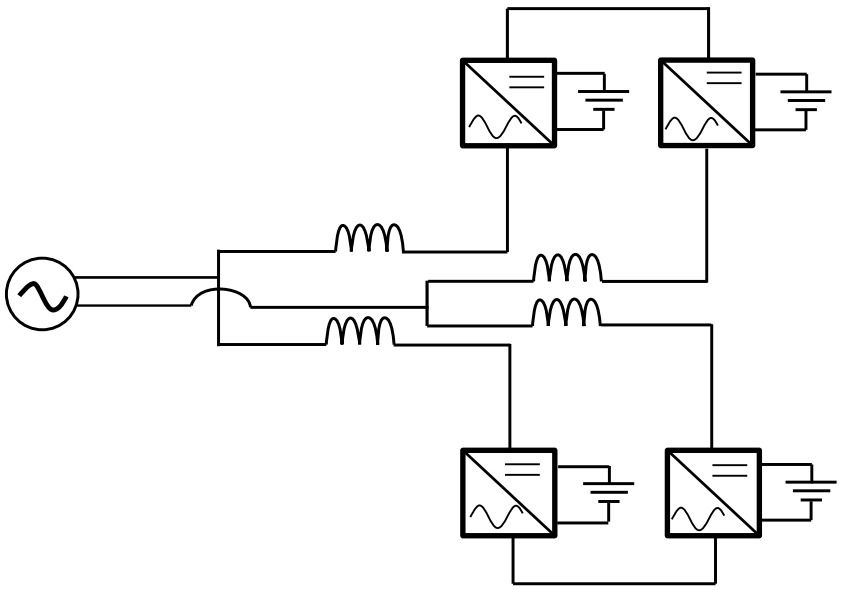

Figure 2. Modular Multilevel Charger (MMC).

Many causes lead to battery failure and understanding the degradation process is essential in minimizing them and intervening as long as possible [12]. Overstress and wear-out are typical causes of failures. The failure by overstress includes temperature thresholds, deep discharge or overdischarge, and partial or incomplete charging [13,14]. Wear-out consists of the degradation over usage related to: Depth of Discharge (DoD) and floatifetime, which are strictly tied to each specific application of the Battery Energy Storage System (BESS).

Research on management of overstress, which consists of limiting the battery usage to protect its integrity, has been widely explored. Because the battery states the maximum

conditions of the usage, a good BESS charger needs to ensure that those values are not exceeded during the cycling processes. In most cases, battery bank chargers ensure that the worst-case stresses remains below the values that were established by the manufacturer. It is worth mentioning that one of the major design challenges of BESS charger is to guarantee this condition for each of the units. Thus, a proper coordinated control for enhancing the BESS operation efficiency is required.

Liang et al. implemented a coordinated charge control in [15] that can be employed by large UPS systems. The main principle is to even the power of each rack according to its rated capacity. The main issue is that its implementation relies on the prior comprehension of the BESS characteristics as well as the battery conditions, such as degradation state, state of charge, age, the temperature of operation, etc. Furthermore, both of the assumptions are harder to be achieved as the battery bank ages. Morello et al. showed, in [16], an implementation of BMS system for controlling a BESS 48V. Despite this contribution, Morello does not address the issue of previously understanding the system characteristics and the BMS is not active and it requires a charger to be controlled. In [17], Chen et al. presented a charge protocol using an accurate estimate of the charging time of a battery and the statistical properties of the charge/discharge patterns, yields an optimal trade-off between aging and quality of service. Other works, such as [18], show systems that are capable of reconfiguring itself to respond to application demands. These systems are the state-of-the-art of the field; however, they still strongly rely on previous understanding of battery stressors, and they focus on charge balance, thus not actively controlling the battery lifetime.

Unlike the large number of researches that were conducted on handling overstress, studies on handling wear-out are still incipient. The purpose of this research field is to rely on controlling the degradation of each battery rather than limiting its use. This can also be done by a BMS [19], but the usage of active BMS, or modular chargers, can boost the control strategy efficiency, as different Depth of Discharge (DoD) can be applied to each unit regarding its condition.

Both of the research fields, overstress and wear-out, have different attributes that can be better explored in a comparative study. Modular chargers could benefit from this comparison, as it enables an enhancement on the active control of each cell or unit. To the best of authorś knowledge, a study comprising such analysis remains a literature gap.

The present work compares the performance of charge control techniques and their implications on the BESS lifetime in an energy-time-shift application using solar power. It presents an overview of the estimation of State of Charge (SoC) and State of Health (SoH). The charge control strategies that are presented in the literature are classified here into two main groups: the Adapted SoC strategy directly linked to the field of overstress management and SoH strategy directly linked to the field of wear-out management. The methodology for comparing the control strategies encompasses an overview of the battery lifetime, charger. and photovoltaic plant models. The adapted SoC and SoH strategies are compared in three distinct simulation cases to illustrate the operation of the BESS in a solar energy time-shift application in different ages and battery technology: a newly formed battery bank (Case 1), a midlife battery bank (Case 2), and a midlife battery bank, in which one battery consisted of different technology and without previous forming (Case 3). The results comprise not only the Capacity Fade, but also Energy Throughput and other stressors, such as current and temperature. Each case is simulated in Simulink/MatLab® using real measure data from a solar power plant. The built-in model provided by MathWorks® was the battery model used.

2. Battery SoC and SoH Estimation Techniques

The State of Charge (SoC) and State of Health (SoH) require estimation and they are indirectly linked from physical quantities, such as current and voltage. The definitions of such parameters are given in the next sections, but, before that, some definitions may be required.

2.1. Battery Charge Related Parameters Definitions

Batteries are electrochemical systems in which electrons and ions are responsible for the charge flow. Thus, the cycling dynamics are governed by Kirchhoff's and Fick's laws, respectively. This subsection lists some battery parameters to better understand the estimation techniques.

Capacity consists of a measurement of the charge that is stored in the battery. It can be calculated as Equation (1)

$$C_p = i.t \tag{1}$$

where C_p is the battery capacity, i is the discharge current, and t is time. One must consider that the discharge time (and capacity) inversely depends on the discharge current. This dependence is described by Peukert [20]. Some nomenclatures of importance regarding capacity are described next:

- The Rated Capacity C_{rtd} consists of the capacity at the rated voltage informed by the manufacturer.
- A fully charged battery has the maximal releasable capacity (C_{rmng}), which can be different from the rated capacity. These differences can be due to deviations in the manufacturing scheme or due to degradation process.

The State of Charge (SoC) consists of the ratio between the available capacity $C_{available}$ and amount of capacity used C_{used}. Note that the available capacity consists of a different value as the C_{rmng}, because the first is corrected by the applied current and the latter is not.

$$SoC = \frac{C_{used}}{C_{available}} \tag{2}$$

The depth of discharge (DoD) is the ratio between the released capacity (used capacity in discharge) and bulk available capacity for the application, refer to Equation (3).

$$DoD = SoC_{mx} - \int_0^t i(\tau)d\tau \tag{3}$$

where SoC_{mx} is the maximum state of charge that is reached in the fully-charged battery, and i is the discharge current.

The Safe Operation Area (SoA) consists of the boundaries that encompass all of the thresholds that protect the integrity of a battery unit [21], such as current, temperature, and voltage.

The State of Health (SoH) consists of the measurement of battery degradation, which is, in essence, multi-factorial.

2.2. State of Charge (SoC) Estimation

The State of Charge can be estimated in various ways. The research and development of new methods to estimate this variable has been a major challenge because of the complex electrochemical reactions and degradation process. In this section, two of the many estimation options are reviewed because of their facility to be implemented in a control for BESS in operation. One method is called coulomb counting, and the equation can be viewed in (4)

$$SoC = SoC_0 + \frac{1}{C_{rtd}} \int_0^t i(\tau)d\tau \tag{4}$$

where C_{rtd} is the rated capacity, SoC_o is the initial state of charge, and i is the electrical current. Note that the usual value for the equation should be C_{rmng}, which is the real available capacity value of a battery each time, but, normally, this information is not readily available in most BESS systems. In Figure 3, the open-loop for the estimation process can be visualized.

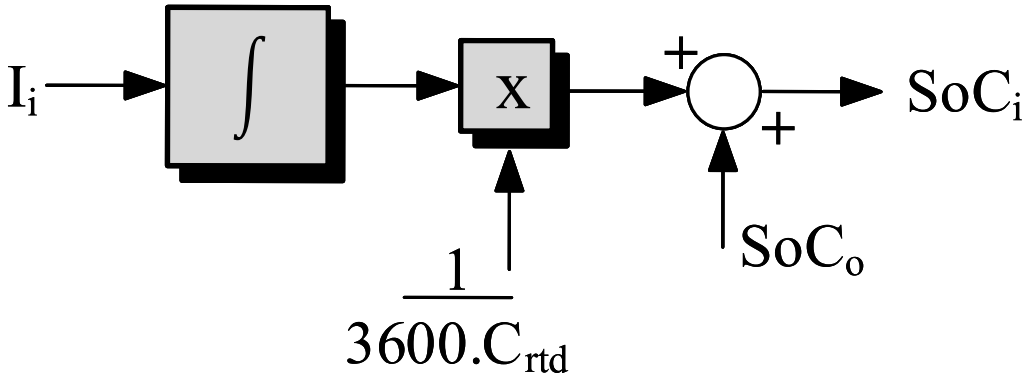

Figure 3. Block diagram for Coulomb counting estimation method.

The main disadvantage of this estimation is that not all current is responsible for the charging process. Side reactions that are present in the battery consume part of that current and the value specific drawn to the charging process and cannot be measured directly. The error due to the current is integrated and it will augment over time. Furthermore, the presence of side reactions is increased as the battery ages. Another method for estimating the State of Charge is through voltage measurement $v(t)$, and the equation wields (5)

$$SoC(t) = \kappa_{bat}.v(t) + SoC_o \tag{5}$$

where κ_{bat} is a parameter that is linked to the battery current, temperature and age. This parameter necessitates extensive tests, which is the main drawback of this approach. The value of the voltage directly relates to the battery state of charge, but some battery types, such as lithium-ion, present a flat OCV (Open-Circuit Voltage) curve, which is harder to be handled in the controller.

Solutions to mitigate these effects have been well addressed in the literature for solutions using fuzzy logic, kalman filter, to reinforcing learning capabilities [22], but the problems discussed previously are still present, as they are inherently related to the battery measurement.

2.3. State of Health (SoH) Estimation

There is no consensus on addressing the State of Health. Studies propose estimation on current dynamics, electrolyte density, and many others [9,23], but the standard protocol to detect the battery age is through capacity fade [24].

The remaining capacity (C_{rmng}) is, to some extent, different from C_{rtd} for a new battery and it declines with time in operation. Equation (6) can be used for evaluating the degradation of a battery.

$$C_{rmng}(t) = C_o - \frac{1}{2NQ_o}\int_0^t |Q_i(\tau)|d\tau \tag{6}$$

where C_o stands for the capacity in the initial stage of the evaluation, N is the equivalent cycle, Q_o stands for the residual charge in the initial stage of the evaluation, and Q_i is the charge. Note that the variable N can be projected to encompass one or various stressors or be directly tied to a specific failure mechanism [25]. The different models of N will ensure, or not, a good prediction of the battery life.

Figure 4 shows the open-loop estimation process. Note that the term inside the integral is a charge, and then the same equation can be rewritten as the double integral of current.

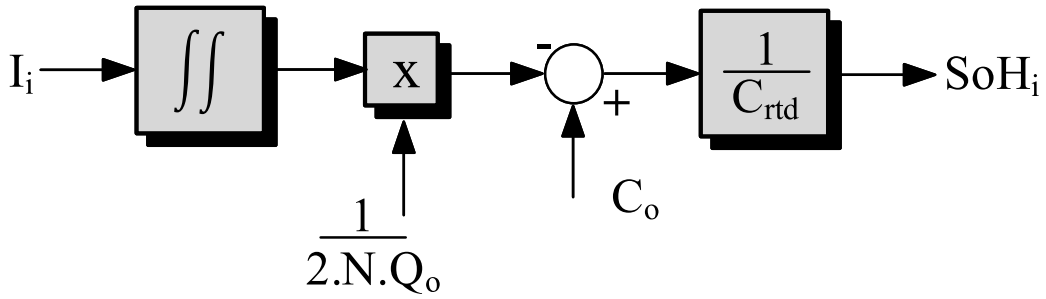

Figure 4. Block diagram for Capacity fade method.

3. Control Strategies for Battery Chargers

Modular charger, as stated in Section 1, is composed of multiple chargers for each battery or unit, as seen in Figure 5. The control strategy is decentralized, as each converter is responsible for a specific unit and acts upon it. The operation of the system is upheld by the central control in which the mean variables, i.e., I_m, SoC_m, and SoH_m are set. These variables are calculated, as follows:

$$X_m = \frac{\sum_1^n X_i}{n} \tag{7}$$

in which X stands for the variable of interest.

These terms are used to compare the condition of each battery to the overall battery bank. The actions that are provided by each control strategy will deviate each battery current accordingly.

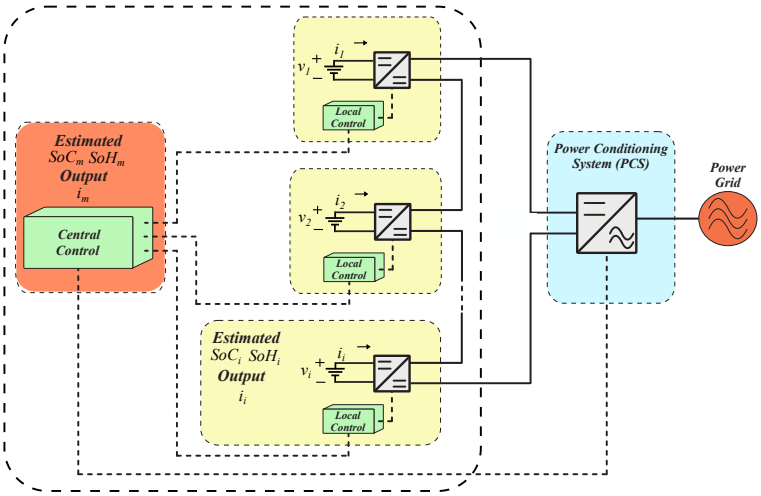

Figure 5. Charger Topology based on a coordinated decentralized control strategy.

The coordinated control of modular chargers units in a bank is proposed to be performed considering a hierarchical control split into three levels, as described below:

- Level 1 (primary control): the primary control level ensures that each unit is charged and discharged accordingly to its particularities. Such control level must also perform the basic and specific functions, like current and voltage control loops, as well as automatic health evaluation.
- Level 2 (secondary control): the secondary level exploits the battery units through coordinated control. Such a control level must also ensure that the electrical levels in the bank are within the required values. It can be devised when considering communication-based functions, or can be implemented in a decentralized fashion using consensus protocol.
- Level 3 (tertiary control): this energy-production level controls the power flow between the modular units and the central charger, which, in turn, goes to the grid.

If this control level is devised in a centralized controller, it can also gather external information, like energy price, local system operator signals, etc, in order to maximize the overall system performance.

Multiple strategies for extending battery lifetime were proposed in the literature as a way to compensate the hazardous charge profiles [26–28]. Advanced charge/discharge strategies not only ensure that each battery unit operates in its Safe Operation Area (SoA), but also optimize the handled energy according to internal and external conditions [29]. These strategies can be classified into two approaches that are covered in the following subsections.

3.1. Adapted SoC Strategy

The objective behind this strategy (Figure 6) is to create different mean variable currents for each battery, depending on its degradation. The equation is visualized in (8).

$$I_i = I_m(SoH_i)(1 + (SoC_m - SoC_i)/k) \tag{8}$$

where I_i is the actual current in the battery, I_m is the maximum current available for each unit, SoC_i is the SoC of each battery, and the SoC_m is the mean SoC of all battery bank. The term SoH_i is the SoH of each battery and k is the controller gain, being responsible for the strength of action of the controller.

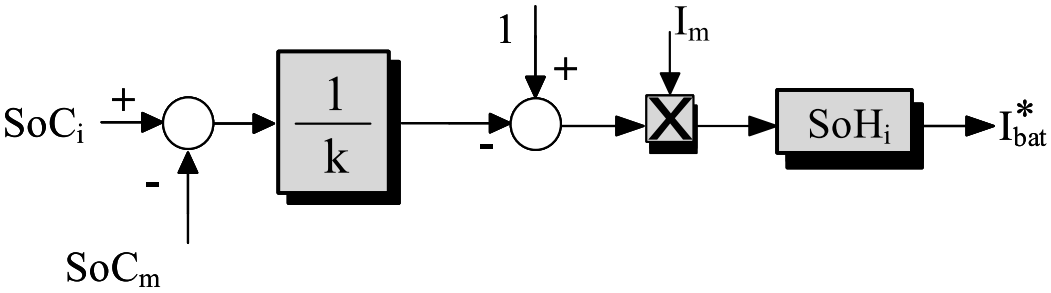

Figure 6. Block diagram of the adapted SoC strategy.

An important aspect to note is that no management of the overall bank lifetime is performed, only overstress mitigation. The value of SoH_i creates an imbalance that is enhanced as the bank ages. Thus, a decline in the charge efficiency is expected as the battery bank ages.

Several authors have proposed solutions using this method [30], and the differences between them are related to estimation techniques and not in the control method.

Y. Li and Y. Han, in [31], present a topology of an electronic battery, in which the main goal is to equalize the battery units based on average battery parameters values. However, in such a proposal, the parameter deviations in each battery are not taken into account. A decentralized control strategy is required to accommodate the battery limits. The implementation of a decentralized control strategy is challenging because the standard control variables are independent of the operation of the system and some constraints must be applied for the operation of the system.

Kim et al., in [32], show the application of these strategies combined with various charge profiles, like CC-CV, pulse charge in order to extend the battery life.

Howey and Frost, in [33], show this application in a decentralized control topology using an MMC converter. The usage of this topology as a second-hand battery approach was conducted by Liu et al. [34]. Another point to note is that the gain k, increases or decreases the speed of the charge balancing scheme [35]. In other words, no effect on the battery lifetime is expected by varying this gain.

3.2. SoH Strategy

This strategy consists of converging the overall lifetime of a bank (Figure 7) [36]. The concept is to converge each of the batteries SoH_i to the mean value of the bank. The equation is visualized in (9).

$$I_i = I_m(1 - (SoH_m - SoH_i)/k) \tag{9}$$

where SoH_m is the mean value of the state of health, the other terms were already addressed in the last subsection. The strategy does not balance the cells and, thus, each battery is expected to reach its final voltage in different times [37].

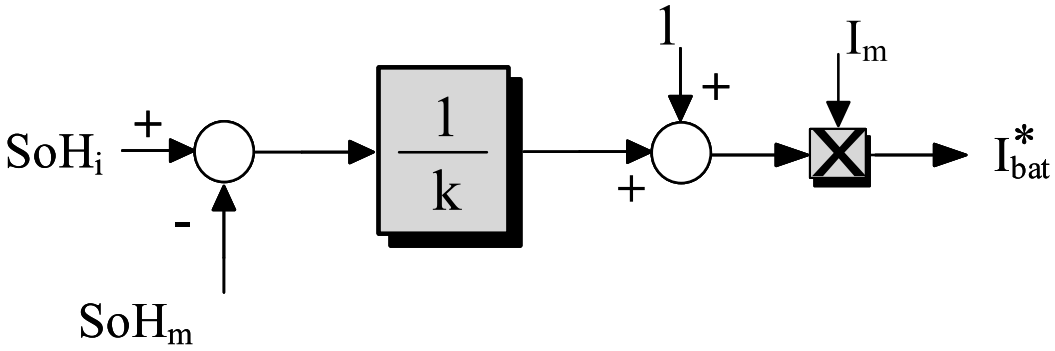

Figure 7. Block diagram of the SoH strategy.

4. Materials and Methods

Because studies that are related to battery banks are, in essence, multi-factorial, control strategies effects can be masked by, for example, charge profile, battery models, and variable estimation techniques, among other factors. In these cases, ensuring a better correlation between the results and control strategy is advantageous, which is provided by the use of simulations, since this approach simplifies models.

In this section, a detailed description of the battery lifetime modeling is present as well as the photovoltaic (PV) system and modular charger model.

4.1. Battery Lifetime Modeling

Reliability is a known concern for battery systems. Various models have been developed [38] over the years, with applications ranging to specific failure mechanisms, such as electrolyte diffusion [39]. Aiming to evaluate the mentioned topologies, the *Matlab/Simulink®* platform is chosen, because the built-in battery model provided has implemented real battery estimations that cover the research needs once the main goal is to address the control strategy performances.

The remaining capacity (C_{rmng}) of each battery cell has a dispersion to its rated capacity of the Li-ion battery pack. The values for the calculation of that dispersion were obtained, as shown in [40]. The aging effect is set through the number of equivalent cycles, as shown in Equation (10)

$$N(n) = H \cdot (DoD)^{\xi} \cdot (I_{dis}(n))^{\gamma_1} \cdot (I_{cha}(n))^{\gamma_2} \tag{10}$$

where,

- $N(n)$ is the number of equivalent cycles
- DoD is the cycle depth of discharge
- $I_{dis}(n)$ is the discharge current
- $I_{cha}(n)$ is the charge current
- H,γ_1,γ_2 and ξ are constants determined experimentally by the mathworks team for a specific battery type and age.

One important thing to note is that all stressors, DoD, $I_{dis}(n)$, and $I_{cha}(n)$, are independent of the others and they affect the battery lifetime model. This idea has been backed up by [41]. Another point is that some important stressors are missing (cell temperature and terminal charge voltage refer to Section 1). For the analyses that were conducted herein, these stressors are evaluated, but, qualitatively, as those stressors do not reflect in the lifetime results. Further information can be found in the *Matlab/Simulink®* documentation [42].

4.2. Battery Bank Application

The application in which the battery bank is used has a strong influence on battery degradation. For a fair comparison of each control strategy, the application and used capacity of the battery bank needs to be the same mean-wise, as well as the dispersion of each battery in the battery bank. The application chosen is Energy time shift [43] for a PV system, the same charge released is deployed for the system, and the same mean DoD_m is adopted for both of the strategies. The PV power plant considered in this study has the following characteristics:

- location: the site is located in the School of Engineering at Federal University of Minas Gerais (UFMG);
- 19°52′10.81″ S 43°57′42.01″ W. Altitude 808 m;
- total peak power: 37.2 kW;
- nominal peak power: 36.0 kW;
- expected energy delivered to the grid: 53.847 kWh/year;
- total area: 439 m^2, and area covered by PV modules = 257 m^2;
- number of PV modules: 154; and,
- each PV module peak power: 245 W.

The sizing of the battery bank was performed, as detailed in [44]. The battery bank was dimensioned for a DoD_m of 40%, as shown in Figure 8. The data of the measurement of the PV power plant during a month were applied to System Advisory Model (SAM) software [45]

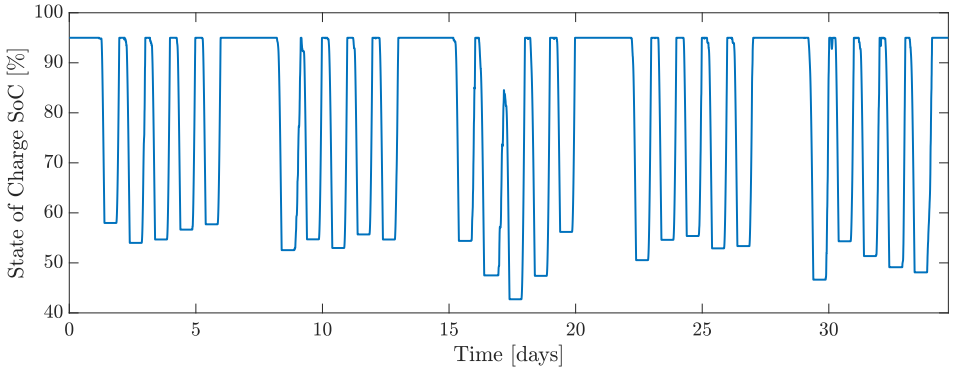

Figure 8. Excursion of the SoC during a month.

The intermittence of the source needs to be taken into account, as the study is about a PV charger. Normally in lifetime analysis, the battery is considered to be fully charged during each cycle; for the reason specified before, this assumption cannot be always respected. Thus, a change on the Equation (3) is required. Thus, Equation (11) yields.

$$DoD = SoC_{min} + \int_0^t I(\tau)d\tau \tag{11}$$

In this equation, it is assumed that the starting point of the charge or the endpoint of discharge SoC_{min}. Thus, the DoD_m yields, as observed in Figure 9.

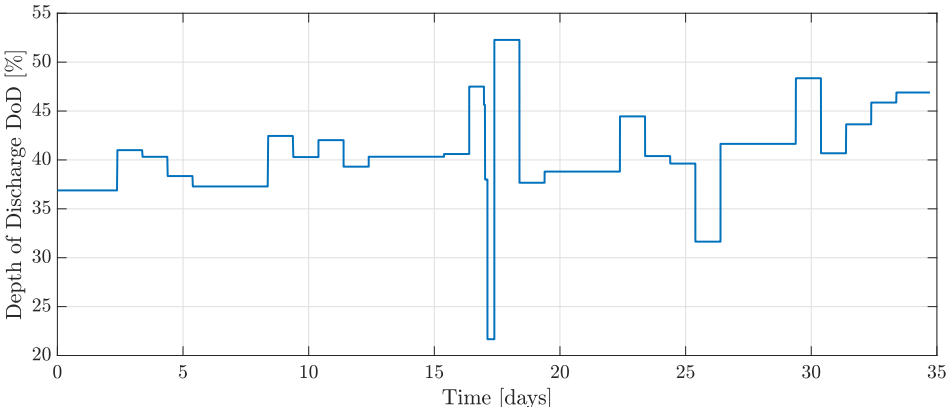

Figure 9. DoD corrected during a month.

One can note that the variation of the DoD_m throughout the month. This makes the solar charger application different from the grid-charged ones. Observe that the ranging of the SoC variation goes from 40% to 80%. This means that the battery is operating on its ohmic region and no limiting in the battery voltage is required.

4.3. Modular Charger Model

The MCC charger topology consists of associating each battery to a dedicated dc-dc converter. The control strategy is separated into local and central. The PCS is responsible for the central control, while each module is responsible for the local control.

A hierarchical control of several modular units is necessary, as stated in Section 1. This paper focuses on the primary control (first level). For this analysis, a converter in a steady-state is implemented as ideal current sources. The control utilized is the current mode and, for a modular charger, each current of the units wields Equation (12).

$$I_{b_i} = \frac{1}{n} I_r \tag{12}$$

where n is the number of units in the battery bank, I_{b_i} is each battery current and I_r is the actual current flowing through the system.

5. Simulation Results

This section compares the control strategies that are described in Section 3. The simulation results demonstrate the behavior of three lithium-ion batteries in a system that is composed of an MCC charger powered by a PV for the application of energy time shift, refer to Section 4.2. Section 5.1 shows the recharge profile to be applied to the battery for the analysis of the strategies. Section 5.2 shows the effect of gain for both strategies. Section 5.3 shows the effect of the estimation process on each strategy. Section 5.4 shows the strategies being analyzed through three case studies to evaluate each strategy in different battery bank conditions.

5.1. Charge/Discharge Profile

For an energy time-shift application, the battery is charged with solar power. The application consists of charging the battery in 6 h, since this is an average daily value for sunbathing and discharge in 3 h. This is a condition that consists of the high rate of energy price. Figure 10 shows the charge/discharge profile, and voltage and current are plotted in different axis for a clearer view. The Simulink battery model of a 5.4 Ah lithium-ion battery ($LiCoO_2$) is charged with 0.9 A (1/6 C) and discharge with 1.8 A (1/3 C).

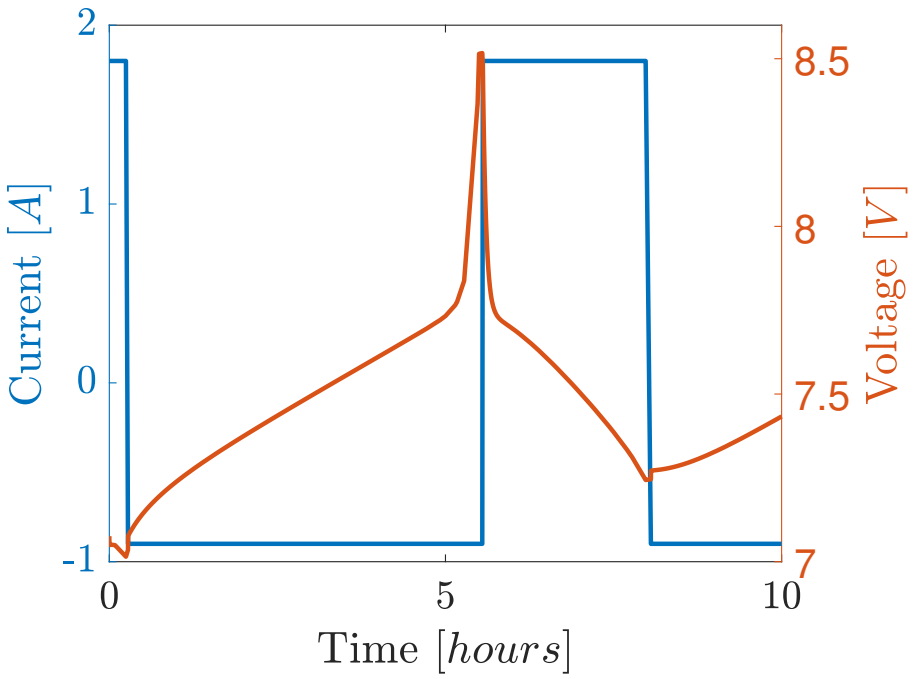

Figure 10. Charge/discharge profile: current and voltage.

Table 1 shows the parameters of the built-in thermal model that was deployed in the MatLab/ Simulink® environment. This model is used throughout the simulations and the parameters were not changed.

In Figure 11, the state of charge and cell temperature are shown. The maximum cell temperature reaches 28.5 °C at the end of discharge. Because the charge profile is one key component in battery degradation, the same profile is used for the comparison of the strategies.

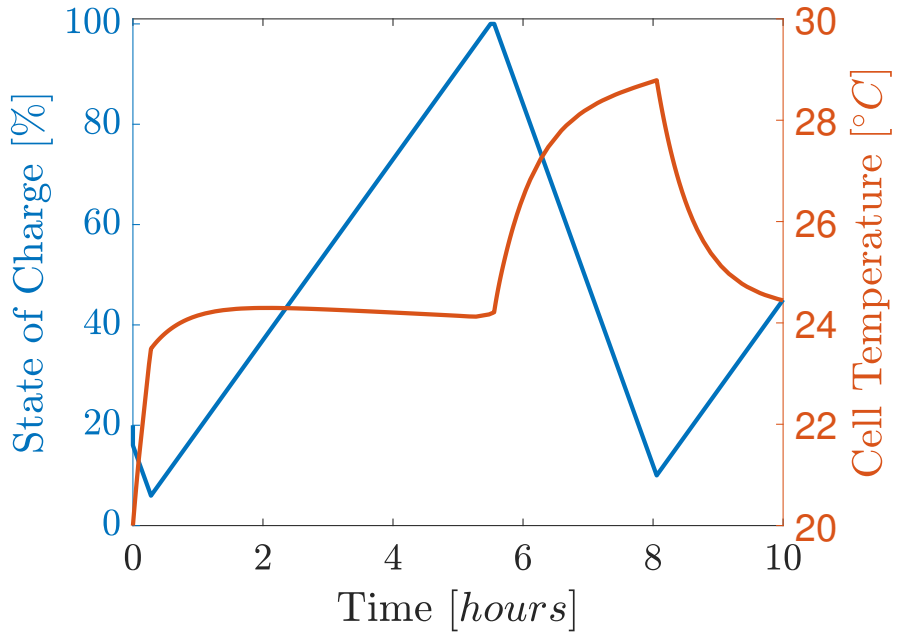

Figure 11. Charge/discharge profile: SoC and cell temperature.

Table 1. Batteries Thermal parameters.

Parameters	Values
Thermal resistance [°C/W]	0.6
Thermal time constant [s]	2000

The results of the recharge profile provide insights into the battery lifespan. The discharge current affects the degradation process more significantly due to its higher value when compared with the recharge current, as referred to in Equation (10). It is worth noting that the battery has not been largely stressed, since the limits of the Safe Operation Area (SoA) have been respected. In this case, the battery was fully recharged, which is rarely the situation in photovoltaic systems.

5.2. Effect on Gain k

On each strategy, the gain, named k in Equations (8) and (9), modifies the velocity on the time in which the desired setpoint is reached. This section shows the amount of control that each strategy has over the battery lifetime. For the evaluation of the gain in each strategy, 1000 h with the Depth of discharge was used according to Figure 12. The MatLab/Simulink® battery model is used, and the parameters of each battery are shown in Table 2.

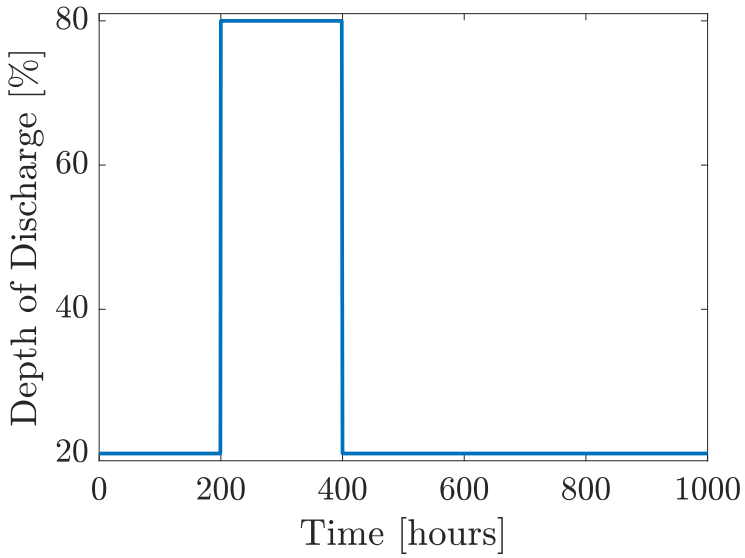

Figure 12. Depth of Discharge for 1000 h simulation.

In Figure 12, a varying Depth of Discharge is used to emulate a battery bank charged by PV system, as discussed in Section 4.2.

Table 2. Batteries parameters.

Parameter	Battery 1	Battery 2	Battery 3
Nominal voltage	7.2 V	7.2 V	7.2 V
Rated capacity	5.4 Ah	5.4 Ah	5.4 Ah
Remaining Capacity	5.37 Ah	5.35 Ah	5.54 Ah
Initial SoC	20%	30%	10%
Number of Cycles [a]	0	0	0

[a] The Number of Cycles in the begining of the simulation.

The first strategy is based on an SoC balancing scheme, and the gain is related to the convergence velocity of the individual SoC values. No difference in the remaining capacity by varying the gain factor is observed, as can be noted in Figures 13–15. It means that no active control of the lifetime can be done with this strategy.

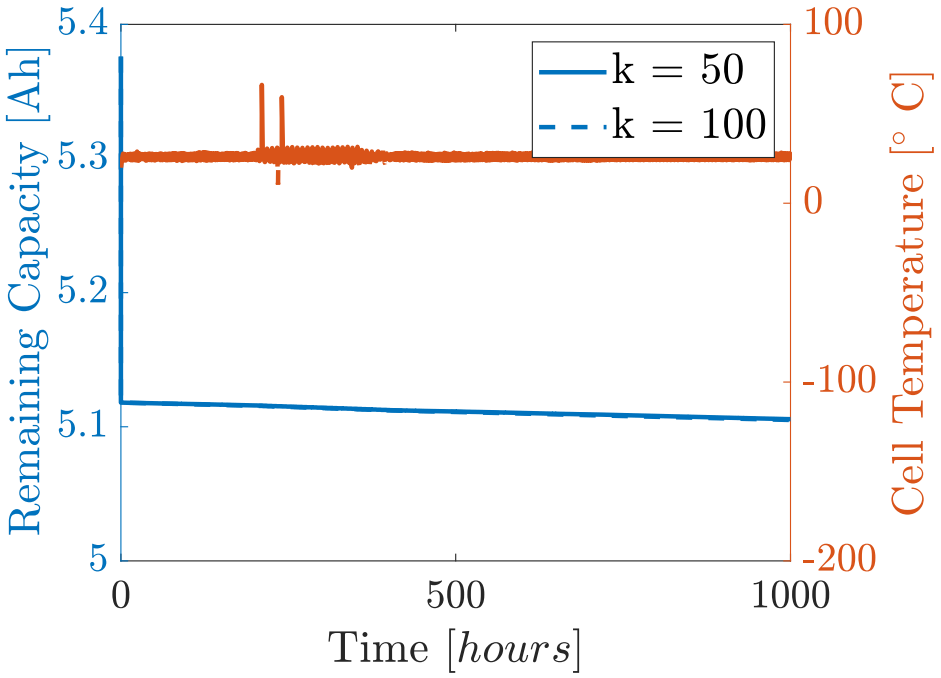

Figure 13. Advanced SoC: Effect of the gain k on Battery 1.

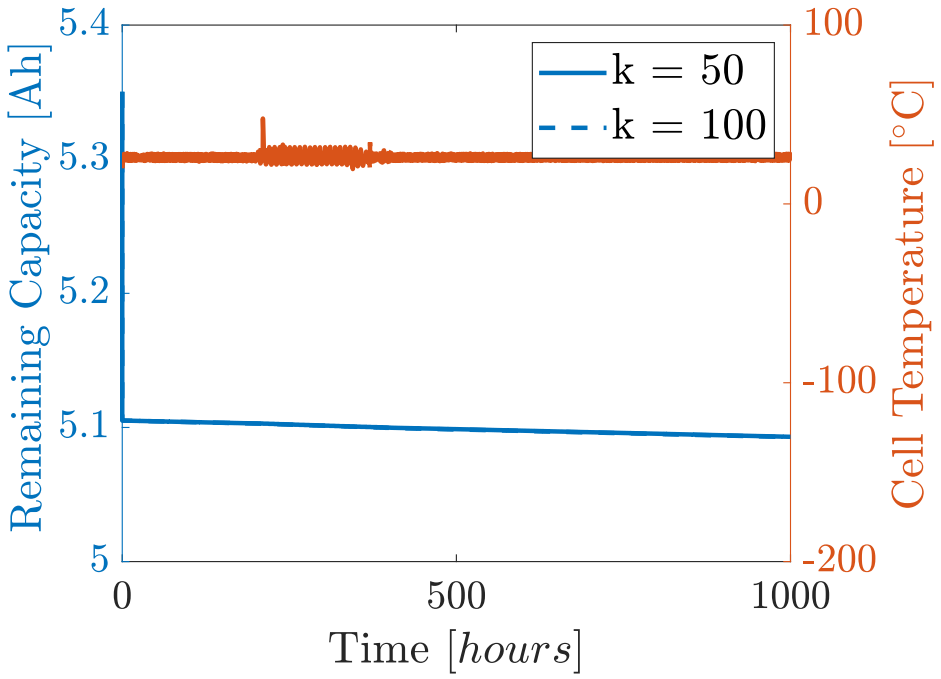

Figure 14. Advanced SoC: Effect of the gain k on Battery 2.

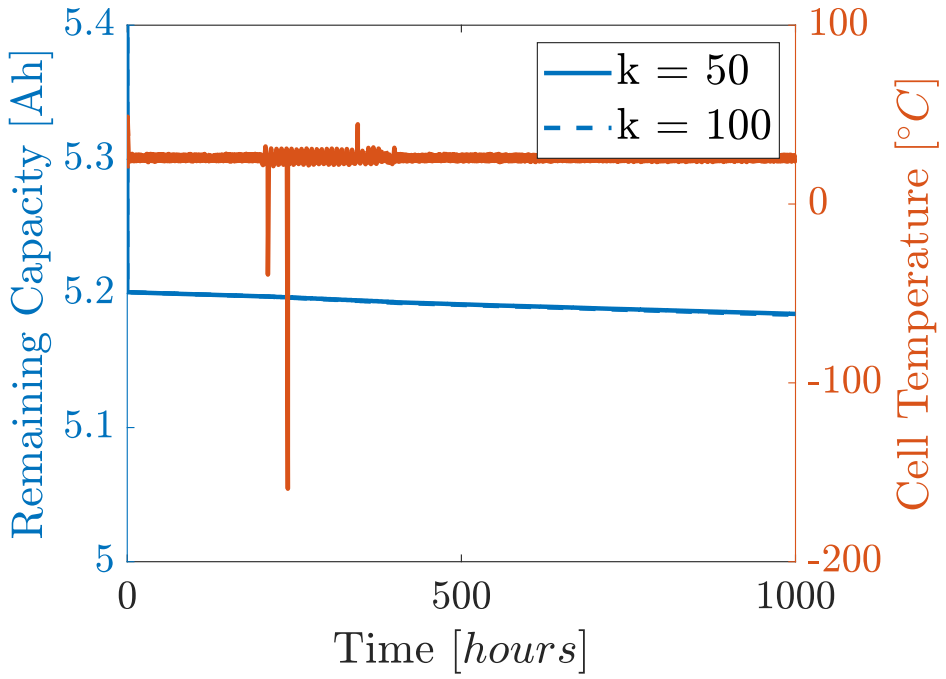

Figure 15. Advanced SoC: Effect of the gain k on Battery 3.

Note that the time of the step in the depth of discharge creates an oscillation in the battery temperature; refer to the oscillating temperature and the differences in scale for each battery (Figures 13–15). Those oscillations in temperature can reach values beyond the safety threshold (SoA) and other methods for damping these values may be applied. Thus, a change in the charge/discharge profile is required.

Contrary to the first strategy, the gain k impacts the overall lifetime of the bank, as can be visualized in Figures 16–18. Clearly, this approach permits the active control of the battery lifetime, which manages the wear-out.

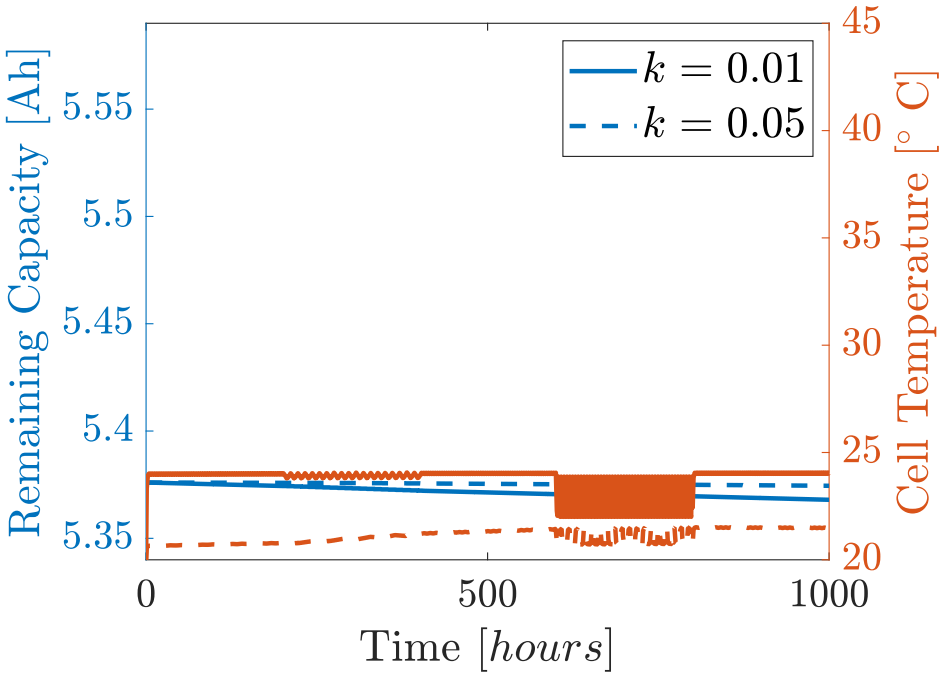

Figure 16. SoH: Effect of the gain k on Battery 1.

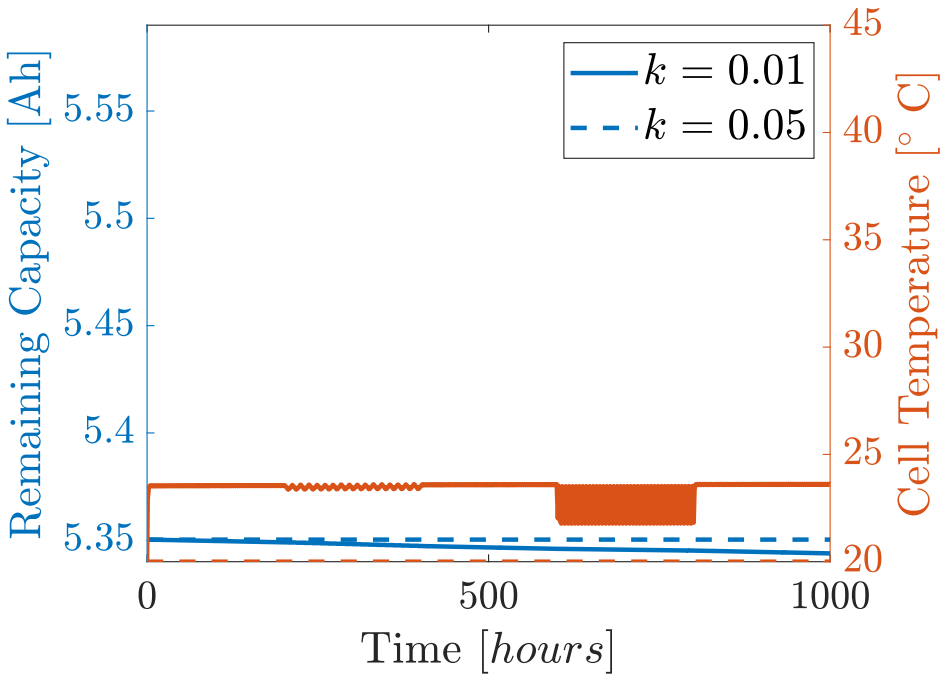

Figure 17. SoH: Effect of the gain k on Battery 2.

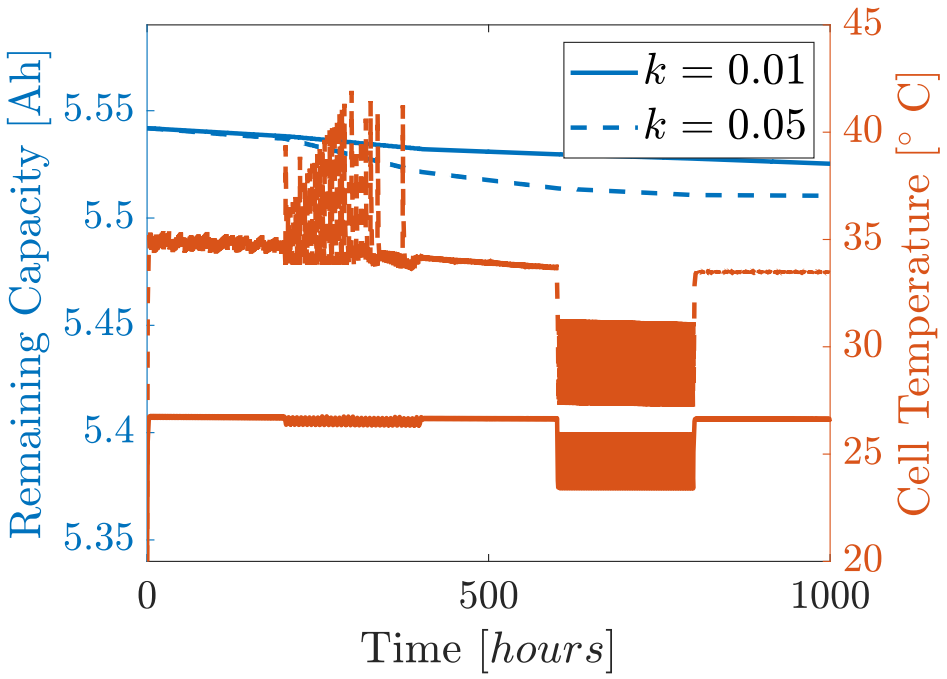

Figure 18. SoH: Effect of the gain k on Battery 3.

A major drawback is the Safe Operation Area (SoA) threshold (refer to Section 1), specifically the battery temperature, as can be seen in Figures 16–18. Depending on the k value, limitations in the battery current should be made to limit the temperature rise. It can be noted that battery 3 has reached the highest value of temperature among the three units, which is dangerous for Li-ion batteries. Another interesting point is that battery 2 with gain $k = 0.05$ does not charge or discharge, due to the differences between the remaining capacity of each cell. Because the conditions of the battery's degradation change overtime and at a different rate, a tune condition for batteries in their prime, new battery with

low disparity, can drastically change as the bank ages. Thus, proper auto-tuning might be needed.

This section compares the effects of the control action of the two analyzed strategies on the battery lifespan. The results showed that the adapted SoC strategy did nto affect the battery lifetime. This implies that any possible increase in the system's lifespan must be given by other factors, such as the recharge profile. In the case of the SoH strategy, the control action directly influenced the battery bank lifetime. Thus, the active management of the battery bank allows either extracting more energy under suitable solarimetric conditions or reducing the energy that is extracted to extend the BESS lifespan.

5.3. Effect of the Estimation of SoH and SoC

The diagram blocks of each strategy is shown here in a closed-loop for one battery in Figures 19 and 20. The current I_m is the set current by the central charger. The variables with the index e (SoC_{ei}, SoC_{em}, SoH_{ei}, and SoH_{em}) are the estimated variables calculated, as shown in Section 2.

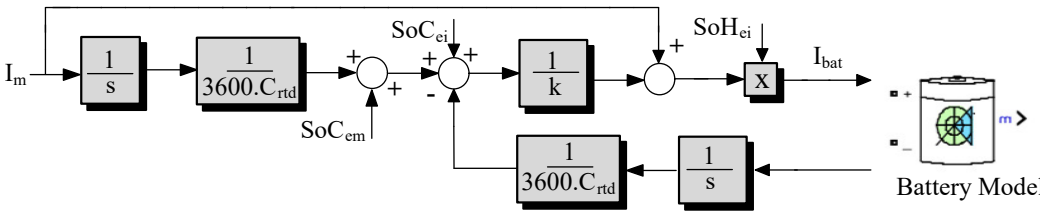

Figure 19. Advanced SoC diagram block.

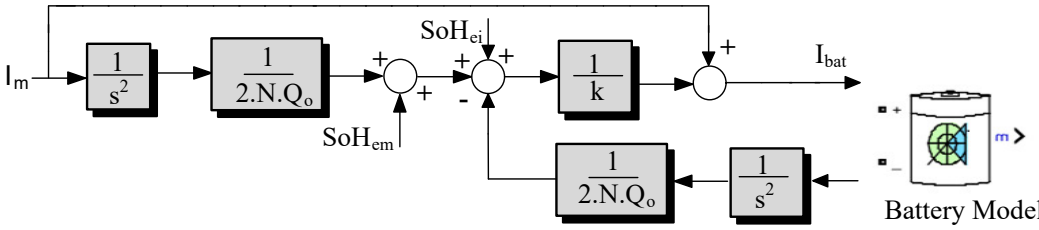

Figure 20. Advanced SoC diagram block.

There is no feedback reinforcing the control of the desired variable (SoH and SoC), as can be observed by the control loops for both strategies. It is necessary that the estimation mechanism be as reliable as possible, but the absence of a direct measurement for this variable makes a direct feedback loop impossible to be achieved. The solutions included in the literature are estimators, such as Kalman filter, Opinath, and others. In this subsection, the operation of 50 h is analyzed looking at stressors mechanisms for each strategy. For this analysis, a fixed DoD of 80% is used and the same battery bank as in Table 2. Because the objective here is to analyze the effect of estimated variables on the control strategy, a simpler estimated technique has been chosen for this analysis.

5.3.1. Adapted SoC

Figures 21 and 22 show the results of the SoH control strategy.

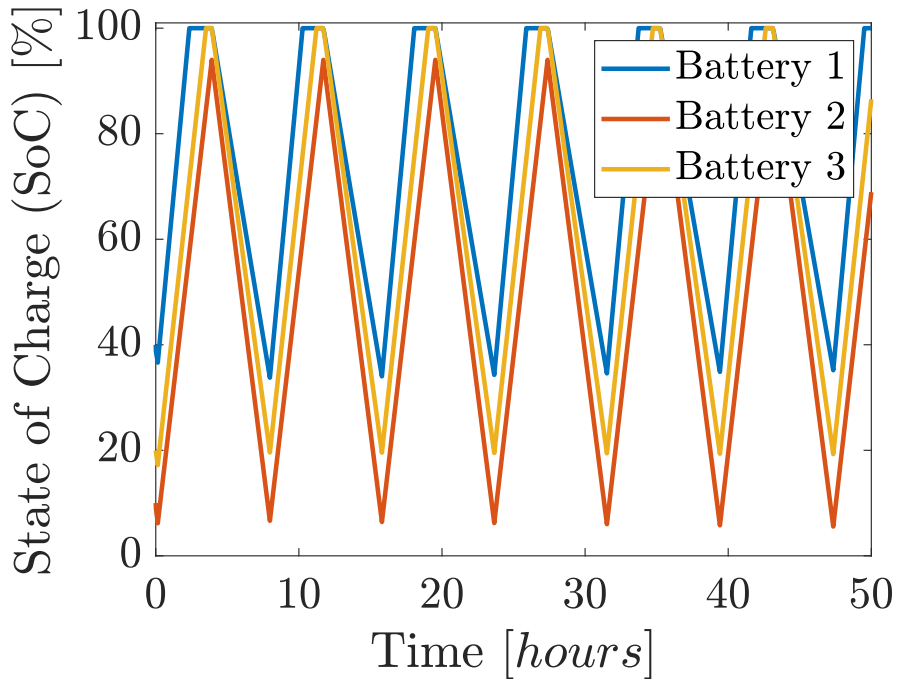

Figure 21. State of Charge Advanced SoC.

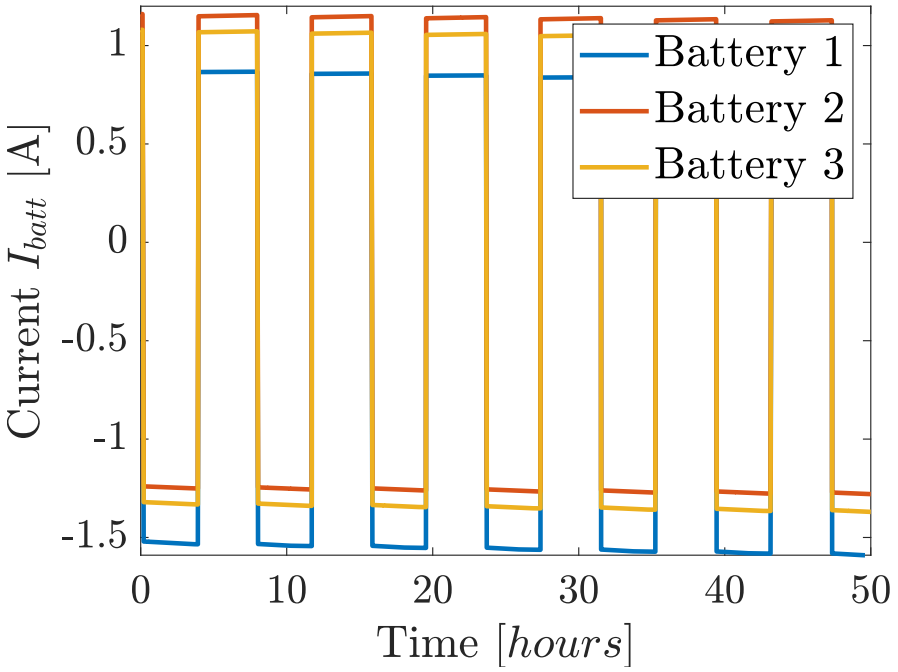

Figure 22. Current values for the advanced SoC strategy.

As can be analyzed, each battery is charged and discharged with different current values, and achieves different final values of SoC at end of charge and discharge accordingly. In Figure 23, one can note that the reference value has been achieved, although each battery SoC is not controlled accordingly.

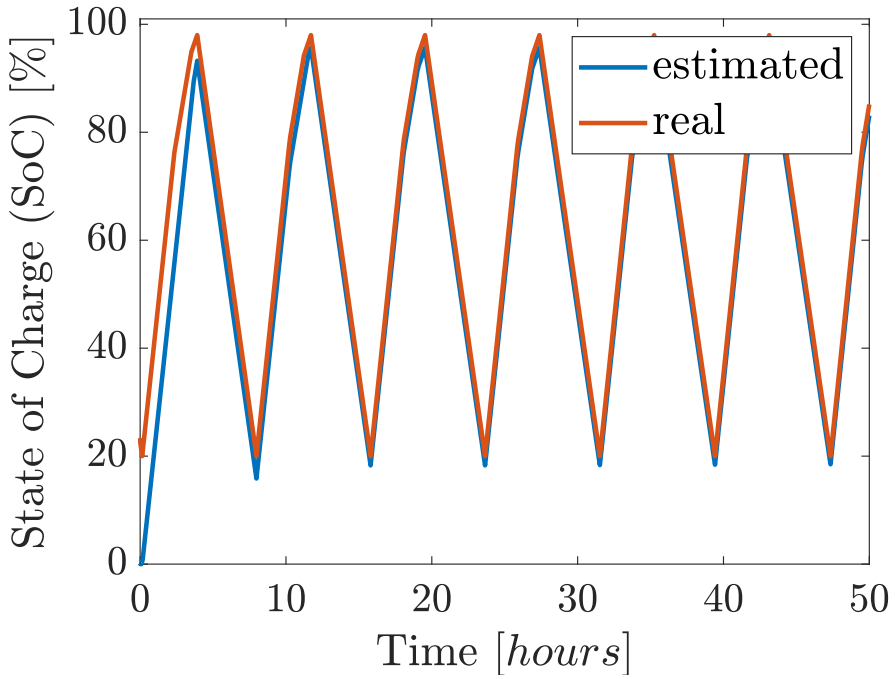

Figure 23. SoC estimation for the advanced SoC strategy.

5.3.2. SoH

Figures 24 and 25 show the results of the control strategy.

As can be viewed in each battery, the value of charge and discharge current remains the same and thus each SoC value. In Figure 26, note that the reference value has not been achieved, making an offset that increases at each iteration making this strategy more complex to be dealt with.

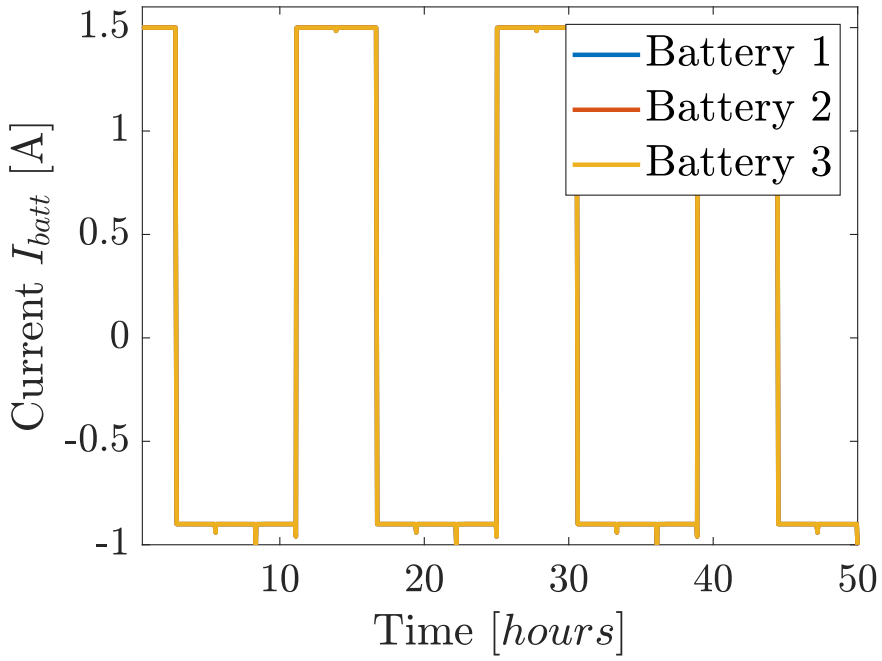

Figure 24. Current values considering the SoH strategy.

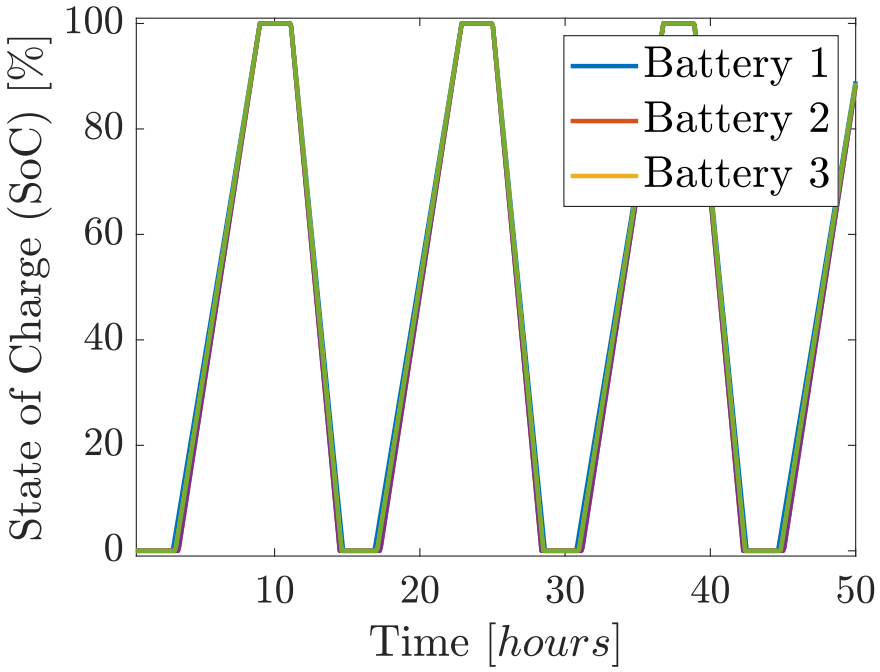

Figure 25. State of Charge values considering the SoH strategy.

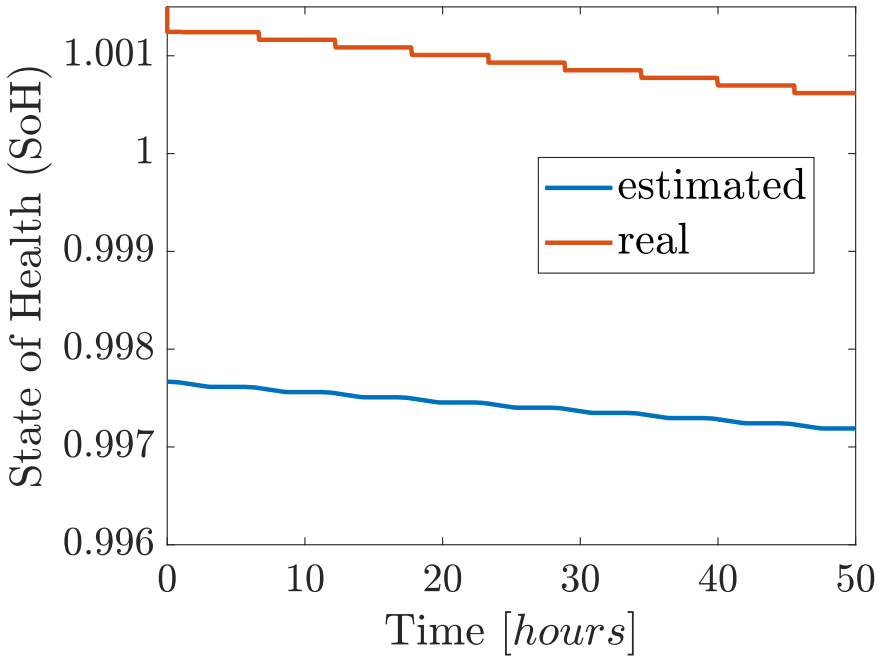

Figure 26. State of Health Estimation considering the SoH strategy.

The control strategies analysed cannot correct errors due to the problems inherent to estimation. It would be necessary to insert a feedback loop to control eventual errors and deviations from estimations. This problem is especially critical for the SoH variable, since it is measured at a lower sampling rate than the SoC, which prolongs the action of the error.

In the simulation, the estimated values (SoC_{em}, SoC_e, SoH_{em}, SoH_e) were different from the initial values that were provided by the battery model, to mimic the inaccuracy of the estimation values. While the SoC error was minimized during the simulation, the SoH error was not.

5.4. Lifetime Analysis

Some of the stressors are not present in the Simulink lifetime model, as observed in the Section 4.1 on battery lifetime modeling. Thus, an evaluation of each stressor needs to be taken into account separately. The evaluation of the current, cell temperature, and voltage is dealt with herein. The mean value of each of the stressors, as well as their peaks and wells, are enough for an in-depth evaluation of each strategy. Figure 1 shows the electric circuit considered in the simulation results with three batteries in series connected to the grid through a central charger. This simulation analyzes the degradation of a modular bank for a month with the corrected DoD calculated, as in Equation (3). Table 3 presents the gain of each control strategy.

Table 3. Gain of the control strategies.

Strategies	k
adapted SoC	100
SoH	0.2

The gain values of each strategy are chosen to minimize dangerous battery effects (refer to Section 5.2). The two strategies are analyzed with three distinct cases:

1. New battery bank with batteries of the same technology.
2. MidLife battery bank with batteries of the same technology.
3. MidLife battery bank with one changed battery of different technology and new.

These cases emulate different conditions in the battery bank as it progressively ages and what implications the control strategy has in its results.

5.4.1. Case 1: New Bank

To compare the control strategies, a bank that is composed of three modular charger based on lithium-ion batteries ($LiCoO_2$) is simulated at Matlab/Simulink® environment. The Simulink® battery model based on [46] is used. The batteries parameters values are shown in Table 4.

Table 4. Batteries parameters.

Parameter	Battery 1	Battery 2	Battery 3
Nominal voltage	7.2 V	7.2 V	7.2 V
Rated capacity	5.4 Ah	5.4 Ah	5.4 Ah
Remaining Capacity	5.37 Ah	5.35 Ah	5.54 Ah
Initial SoC	30%	30%	30%
Number of Cycles	0	0	0

In this simulation, all of the batteries are considered to be formed, which is, they have reached their full remaining capacity. Table 5 shows the final value of the capacity for each strategy.

Table 5. Remaining Capacity at the end of the month of simulation: Case 1.

Capacity [Ah]	Battery 1	Battery 2	Battery 3
adapted SoC	5.24	5.22	5.36
SoH	5.23	5.21	5.36

Tables 6–8 show the minimum, average, and maximum value of the stressors of each battery for both of the strategies.

Table 6. Battery 1 during a month of simulation: Case 1.

	Voltage [V]			Current [A]			Temperature [°C]		
	min	**avg**	**max**	**min**	**avg**	**max**	**min**	**avg**	**max**
adapted SoC	7.11	7.4	7.63	−1.2	0.171	2.47	20.0	25.8	29.5
SoH	7.11	7.41	7.63	−0.9	0.0535	1.8	20.0	25.8	28.7
gain	0	1.001	0	0.75	0.31	0.73	0	0	0.973

Table 7. Battery 2 during a month of simulation: Case 1.

	Voltage [V]			Current [A]			Temperature [°C]		
	min	**avg**	**max**	**min**	**avg**	**max**	**min**	**avg**	**max**
adapted SoC	7.12	7.4	7.64	−1.21	0.178	2.48	20.0	25.8	29.4
SoH	7.12	7.41	7.63	−0.9	0.0553	1.8	20.0	25.8	28.7
gain	0	1.001	0.999	0.744	0.311	0.726	0	0	0.976

Table 8. Battery 3 during a month of simulation: Case 1.

	Voltage [V]			Current [A]			Temperature [°C]		
	min	**avg**	**max**	**min**	**avg**	**max**	**min**	**avg**	**max**
adapted SoC	7.09	7.39	7.63	−1.24	0.226	2.55	20.0	25.7	29.3
SoH	7.1	7.39	7.62	−0.9	0.0201	1.8	20.0	25.6	28.4
gain	1.001	0	0.999	0.726	0.089	0.706	0	0.996	0.969

The values in the simulation show similar results for the voltage and temperature span, but the current gives an advantage to the adapted SoC strategy. Note that the variation of parameters within the batteries in this condition is minimum, which is probably due to the battery bank being new and of the same battery technology.

5.4.2. Case 2: Mid-Life Bank

In this simulation, the battery parameters are changed in the number of cycles. When considering that this battery has a target number of cycles of 1500, the half-life is 750. Table 9 shows the battery parameters for this analysis. A change in the remaining capacity parameter is noted; this is only due to the model degradation and dispersion remaining the same.

Table 9. Batteries parameters for Case 2.

Parameter	**Battery 1**	**Battery 2**	**Battery 3**
Nominal voltage	7.2 V	7.2 V	7.2 V
Rated capacity	5.4 Ah	5.4 Ah	5.4 Ah
Remaining Capacity	5.04 Ah	5.15 Ah	5.2 Ah
Initial SoC	30%	30%	30%
Number of Cycles	750	750	750

The simulation results are shown in Tables 10–12.

Table 10. Battery 1 during a month of simulation: Case 2.

	Voltage [V]			Current [A]			Temperature [°C]		
	min	**avg**	**max**	**min**	**avg**	**max**	**min**	**avg**	**max**
adapted SoC	7.14	7.41	7.64	−1.14	0.167	2.36	20.0	25.5	28.9
SoH	7.14	7.42	7.63	−0.9	0.341	1.8	20.0	26.2	28.6
gain	0	1.001	0.999	0.789	2.042	0.763	0	1.027	0.990

Table 11. Battery 2 during a month of simulation: Case 2.

	Voltage [V]			Current [A]			Temperature [°C]		
	min	**avg**	**max**	**min**	**avg**	**max**	**min**	**avg**	**max**
adapted SoC	7.14	7.41	7.66	−1.16	0.17	2.37	20.0	25.5	29.1
SoH	7.14	7.42	7.63	−0.9	0.337	1.8	20.0	26.1	28.6
gain	0	1.001	0.996	0.776	1.982	0.759	0	1.023	0.983

Table 12. Battery 3 during a month of simulation: Case 2.

	Voltage [V]			Current [A]			Temperature [°C]		
	min	**avg**	**max**	**min**	**avg**	**max**	**min**	**avg**	**max**
adapted SoC	7.12	7.4	7.64	−1.18	0.185	2.42	20.0	25.3	28.8
SoH	7.12	7.4	7.62	−0.9	0.302	1.8	20.0	25.9	28.3
gain	0	0	0.997	0.763	1.632	0.744	0	1.024	0.983

Analyzing Tables 10–12, the differences in the value of the current of both strategies are significant. This is done by the factor SoH_i, multiplying the mid-current I_m.

Table 13 shows the final value of the remaining capacity.

Table 13. Remaining Capacity at the end of the month of simulation.

Capacity [Ah]	**Battery 1**	**Battery 2**	**Battery 3**
adapted SoC	4.99	4.98	5.03
SoH	4.97	4.96	5.0

5.4.3. Case 3: Mid-Life Bank with Different Technology

This analysis evaluates different battery types of Li-ion batteries. The second battery in case 2 is replaced by a new $LiNiO_2$. The parameters can be visualized in Table 14. The second battery is not considered to be formed, which implies that the remaining capacity has not yet achieved its full potential.

Table 14. Batteries parameters for Case 3.

Parameter	**Battery 1**	**Battery 2**	**Battery 3**
Nominal voltage	7.2 V	7.4 V	7.2 V
Rated capacity	5.4 Ah	4.4 Ah	5.4 Ah
Remaining Capacity	5.20 Ah	4.55 Ah	5.18Ah
Initial SoC	30%	30%	30%
Number of Cycles	750	0	750

Tables 15–17 shoe the simulation results of each battery parameter.

Table 15. Battery 1 during a month of simulation: Case 3.

	Voltage [V]			Current [A]			Temperature [°C]		
	min	**avg**	**max**	**min**	**avg**	**max**	**min**	**avg**	**max**
adapted SoC	7.14	7.41	7.65	−1.16	0.191	2.39	20.0	25.5	29.0
SoH	7.14	7.42	7.63	−0.9	0.259	1.8	20.0	26.1	28.6
gain	0	1.001	0.997	0.776	1.356	0.753	0	1.023	0.986

Table 16. Battery 2 during a month of simulation: Case 3.

	Voltage [V]			Current [A]			Temperature [°C]		
	min	**avg**	**max**	**min**	**avg**	**max**	**min**	**avg**	**max**
adapted SoC	7.29	7.59	7.85	−1.04	0.15	2.14	20.0	25.5	28.9
SoH	7.3	7.58	7.82	−0.731	0.152	1.46	20.0	25.4	27.8
gain	1.001	0.999	0.996	0.703	1.013	0.682	0	0.996	0.962

Table 17. Battery 3 during a month of simulation: Case 3.

	Voltage [V]			Current [A]			Temperature [°C]		
	min	**avg**	**max**	**min**	**avg**	**max**	**min**	**avg**	**max**
adapted SoC	7.12	7.4	7.65	−1.16	0.184	2.4	20.0	25.3	28.8
SoH	7.13	7.41	7.62	−0.9	-0.017	1.8	20.0	25.5	28.2
gain	1.001	1.001	0.996	0.776	−0.092	0.75	0	1.008	0.979

Table 18 shows the final value of the remaining capacity. Battery 2 shows an increase in the remaining capacity. This is due to the fact that battery 2 is not fully formed.

Table 18. Remaining Capacity at the end of the month of simulation: Case3.

Capacity [Ah]	**Battery 1**	**Battery 2**	**Battery 3**
adapted SoC	4.99	4.55	5.03
SoH	4.97	4.55	5.0

5.5. Discussion

Previous works have shown new possibilities for advanced chargers topologies with applications ranging from electric vehicles (EV) to standard grid applications. The control strategy employed can be traced back to these two main strategies. An in-depth discussion on the real gain of each strategy is still marginally explored. This analysis needs a battery lifetime model. This type of model is extremely data-driven and extensive lab work is required, both in regards to equipment and time-wise. As the analysis is on control strategy not in the battery itself, a simpler model was chosen. The *Matlab/Simulink®* has options of real batteries implemented and the lifetime model has some limitations, as discussed in the materials and methods section. One important aspect that can be inferred from this work is that the remaining capacity is not a good figure of merit for analyzing these strategies. To correctly evaluate the strategies, one must look beyond the remaining capacity figure. The amount of current that is driven from the battery is directly tied to the degradation and battery usage. For a given application purpose, the battery should be used accordingly, and the maximum available power is wanted. The figures of merit analyzed here are capacity fade, average current and temperature, and energy throughput.

5.5.1. Capacity Fade

Capacity fade consists of the net value obtained by the remaining capacity during the simulation.

The results, as presented in Tables 19–21, show a similar range of the capacity fade through the month analyzed, so other factors must be evaluated.

Table 19. Capacity fade of the control strategies for Case 1.

	Battery1	**Battery 2**	**Battery 3**
adapted SoC	0.136	0.128	0.181
SoH	0.143	0.137	0.185

Table 20. Capacity fade of the control strategies for Case 2.

	Battery1	**Battery 2**	**Battery 3**
adapted SoC	0.389	0.369	0.516
SoH	0.409	0.389	0.541

Table 21. Capacity fade of the control strategies for Case 3.

	Battery1	**Battery 2**	**Battery 3**
adapted SoC	0.389	0.0787	0.516
SoH	0.409	0.0761	0.539

5.5.2. Energy Throughput

This figure of merit shows the amount of energy that is extracted during the analyzed month (refer to Section 4.2). The variations of the data are due to differences in the control strategy. For case 1 (Figure 27), the adapted SoC and SoH strategies present the same results that are linked to the remained capacity values in Table 5. For cases 2 and 3, the adapted SoC deviates from the SoH early in the month simulation (Figures 28 and 29). One important thing to note is that the SoH has a gain of 72.4% for the second case and 36% for the third case. The lower gain of case 3 can be traced by the difference of battery technology with the strategy SoH neglects.

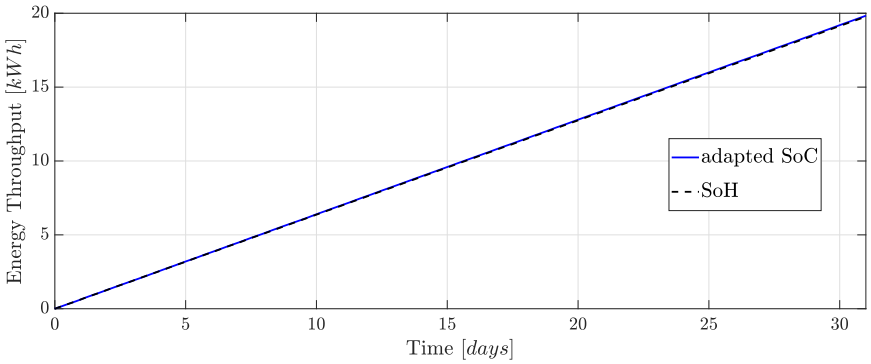

Figure 27. Energy Throughput: Case 1.

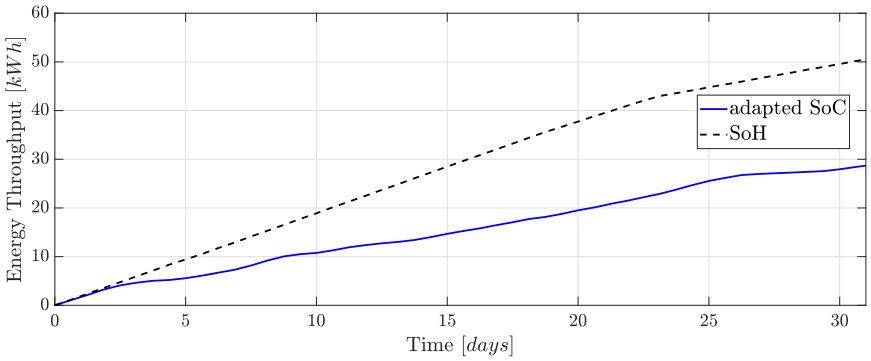

Figure 28. Energy Throughput: Case 2.

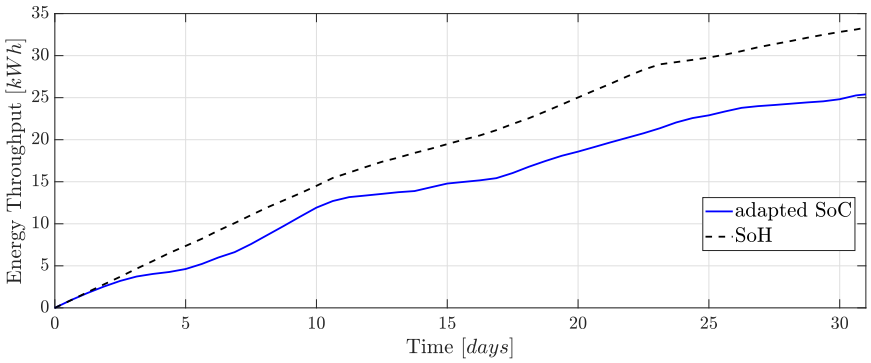

Figure 29. Energy Throughput: Case 3.

This section analyzes the effect of the strategies on the battery lifetime. Firstly, in case 1, there is only a slight variation for the battery voltage, current and temperature values during the simulated month. In contrast, in case 2, which consists of a midlife battery bank, these values present significant variations during time, inasmuch as the adapted SoC strategy drastically limits the operating range of each battery. The difference in energy extracted (Energy Throughput) observed for case 2 reinforces these findings. In case 3, comprising a new un-formed battery (battery 2) and two midlife batteries (batteries 1 and 3), battery 2 increased the value of the remaining capacity for both of the strategies. The rated capacities of battery 2, and batteries 1 and 3, were 4.4 Ah, and 5.4 Ah, respectively. The current that was settled by the central controller was adjusted accordingly. The parameters show that, in both strategies, more current was drained from batteries 1 and 3. Battery 2 drained less current due to its lower capacity. These results show that the SoH strategy lacks the ability to access batteries of different technologies, having a decrease in performance by the added battery

6. Conclusions

Battery banks without proper active charge control lead to deviations in the temperature, current, voltage, and SoC of the units. As a result, the aging process of the batteries is accelerated at different rates. To correct this issue, previous studies have addressed two main strategies: adapted SoC and SoH. This work analyses these two strategies in a PV energy time-shift application considering Capacity Fade and other stressors, such as temperature and current. Simulations in MatLab/Simulink® environment were performed to assess three possible BESS conditions: a new formed battery bank (Case 1), a midlife battery bank (Case 2), and a midlife battery bank in which one battery consisted of a different technology and without previous forming (Case 3). The three cases present similar capacity fade values. The SoH strategy presents an increase of 72.4% in the energy extraction (Energy Throughput) as compared with the adapted SoC strategy in case 2. In case 3, the increase was of 36%. In Case 1, no difference was observed. It is worth noting

that both of the strategies presented problems in the SoH estimation, as no feedback input is available for correcting the estimation. Future works can be performed to address this issue. In addition, the results show that the adapted SoC strategy does not actively control the battery lifetime, as the SoH strategy does. Finally, the SoH strategy is the best approach considering the usage of the battery bank, but applying this strategy in a battery bank consisting of different technologies requires adaptation.

Author Contributions: Conceptualization, N.T.D.F., A.R., D.B. and B.C.F.; methodology, N.T.D.F.; software, N.T.D.F.; validation, N.T.D.F., A.R., D.B. and B.C.F.; formal analysis, N.T.D.F.; investigation, N.T.D.F.; resources, B.C.F.; data curation, N.T.D.F.; writing—original draft preparation, N.T.D.F.; writing—review and editing, N.T.D.F., A.R., D.B. and B.C.F.; visualization, N.T.D.F., A.R., D.B. and B.C.F.; supervision, D.B. and B.C.F.; project administration, B.C.F.; funding acquisition, B.C.F. All authors have read and agreed to the published version of the manuscript.

Funding: This work has been developed under the Research and Technological Development Program of the Electric Energy Sector regulated by ANEEL under the title "*Technical and commercial arrangements for the insertion of energy storage systems in the Brazilian electric sector*", project id ANEEL PD-00553-0046/2016, with Petrobras as the project proponent. The authors also thank the financial support from CAPES, FAPEMIG (grant APQ-02518-16), CNPq (grant 420850/2016-3) and CEFET-MG.

Conflicts of Interest: The authors declare no conflict of interest. The funders had no role in the design of the study; in the collection, analyses, or interpretation of data; in the writing of the manuscript.

Abbreviations

The following abbreviations are used in this manuscript:

BESS	Battery Energy Storage System
DoD	Depth of Discharge
EV	Electric Vehicle
Li-ion	Lithium-ion battery
$LiCoO_2$	Lithium-ion Cobalt dioxide battery
$LiNiO_2$	Lithium-ion Nickel dioxide battery
MCC	Modular Cascaded Converter
MMC	Modular Multilevel Converter
PCS	Power Conditioning System
PV	Photovoltaic
SoA	Safe Operation Area
SoC	State of Charge
SoH	State of Health

References

1. International Energy Agency. *World Energy Outlook 2018*; Technical Report; IEA: Paris, France, 2018.
2. Ferreira, H.L.; Garde, R.; Fulli, G.; Kling, W.; Lopes, J.P. Characterisation of electrical energy storage technologies. *Energy* **2013**, *53*, 288–298. [CrossRef]
3. Liang, M.; Liu, Y.; Xiao, B.; Yang, S.; Wang, Z.; Han, H. An analytical model for the transverse permeability of gas diffusion layer with electrical double layer effects in proton exchange membrane fuel cells. *Int. J. Hydrog. Energy* **2018**, *43*, 17880–17888. [CrossRef]
4. Divya, K.; Østergaar, J. Battery energy storage technology for power systems—An overview. *Electr. Power Syst. Res.* **2009**, *79*, 511–520. [CrossRef]
5. Gao, Y.; Zhang, X.; Cheng, Q.; Guo, B.; Yang, J. Classification and review of the charging strategies for commercial lithium-ion batteries. *IEEE Access* **2019**, *7*, 43511–43524. [CrossRef]
6. Zou, C.; Manzie, C.; Nešić, D. Model predictive control for lithium-ion battery optimal charging. *IEEE/ASME Trans. Mechatronics* **2018**, *23*, 947–957. [CrossRef]
7. Narayanaswamy, S.; Kauer, M.; Steinhorst, S.; Lukasiewycz, M.; Chakraborty, S. Modular active charge balancing for scalable battery packs. *IEEE Trans. Very Large Scale Integr. (VLSI) Syst.* **2016**, *25*, 974–987. [CrossRef]
8. Tashakor, N.; Farjah, E.; Ghanbari, T. A bidirectional battery charger with modular integrated charge equalization circuit. *IEEE Trans. Power Electron.* **2016**, *32*, 2133–2145. [CrossRef]
9. Xiong, R.; Cao, J.; Yu, Q.; He, H.; Sun, F. Critical review on the battery state of charge estimation methods for electric vehicles. *IEEE Access* **2017**, *6*, 1832–1843. [CrossRef]

10. Quraan, M.; Yeo, T.; Tricoli, P.; Korea, S. Design and Control of Modular Multilevel Converters for Battery Electric Vehicles. *IEEE Trans. Power Electron.* **2015**, *8993*, 507–517. [CrossRef]
11. Mukherjee, N.; Strickland, D. Control of second-life hybrid battery energy storage system based on modular boost-multilevel buck converter. *IEEE Trans. Ind. Electron.* **2015**, *62*, 1034–1046. [CrossRef]
12. Kalair, A.; Abas, N.; Saleem, M.S.; Kalair, A.R.; Khan, N. Role of energy storage systems in energy transition from fossil fuels to renewables. *Energy Storage* **2021**, *3*, e135. [CrossRef]
13. Broussely, M.; Herreyre, S.; Biensan, P.; Kasztejna, P.; Nechev, K.; Staniewicz, R. Aging mechanism in Li ion cells and calendar life predictions. *J. Power Sources* **2001**, *97*, 13–21. [CrossRef]
14. Choi, S.S.; Lim, H.S. Factors that affect cycle-life and possible degradation mechanisms of a Li-ion cell based on $LiCoO_2$. *J. Power Sources* **2002**, *111*, 130–136. [CrossRef]
15. Liang, X.; Song, E.; Jiang, F.; Ahuja, N.; Kumar, M. Design considerations for turbo rack with smart battery backup System(BBS). In Proceedings of the 2019 IEEE Applied Power Electronics Conference and Exposition (APEC), Anaheim, CA, USA, 17–21 March 2019. [CrossRef]
16. Morello, R.; Schwarz, R.; Hoedemaekers, E.R.; Habenschaden, F.; DI Rienzo, R.; Roncella, R.; Saletti, R.; Rosca, B.; Steffenhagen, T.; Lorentz, V.R.; et al. Implementation and Test of a 48 v Smart Battery System with Integrated DC/DC Converter. In Proceedings of the 2019 IEEE 28th International Symposium on Industrial Electronics (ISIE), Vancouver, BC, Canada, 12–14 June 2019; Volume 2019, pp. 2440–2445. [CrossRef]
17. Chen, Y.; Bocca, A.; Macii, A.; Macii, E.; Poncino, M. *A Li-Ion Battery Charge Protocol with Optimal Aging-Quality of Service Trade-Off*; Association for Computing Machinery: New York, NY, USA, 2016; pp. 40–45. [CrossRef]
18. Chen, F.; Qiao, W.; Qu, L. A modular and reconfigurable battery system. In Proceedings of the 2017 IEEE Applied Power Electronics Conference and Exposition (APEC), Tampa, FL, USA, 26–30 March 2017. [CrossRef]
19. Weng, C.; Feng, X.; Sun, J.; Peng, H. State-of-health monitoring of lithium-ion battery modules and packs via incremental capacity peak tracking. *Appl. Energy* **2016**, *180*, 360–368. [CrossRef]
20. Doerffel, D.; Sharkh, S.A. A critical review of using the Peukert equation for determining the remaining capacity of lead-acid and lithium-ion batteries. *J. Power Sources* **2006**, *155*, 395–400. [CrossRef]
21. Andrea, D. *Battery Management Systems for Large Lithium Ion Battery Packs*; Artech House: Norwood, MA, USA, 2010.
22. Wei, Z.; He, H.; Pou, J.; Tsui, K.L.; Quan, Z.; Li, Y. Signal-Disturbance Interfacing Elimination for Unbiased Model Parameter Identification of Lithium-Ion Battery. *IEEE Trans. Ind. Inform.* **2020**. [CrossRef]
23. Berecibar, M.; Gandiaga, I.; Villarreal, I.; Omar, N.; Van Mierlo, J.; Van Den Bossche, P. Critical review of state of health estimation methods of Li-ion batteries for real applications. *Renew. Sustain. Energy Rev.* **2016**, *56*, 572–587. [CrossRef]
24. IEEE Standard. *IEEE Recommended Practice for Testing the Performance of Stand-Alone Photovoltaic Systems*; Technical Report; IEEE: Piscataway, NJ, USA, 2004. [CrossRef]
25. De Beer, B.; Rix, A.J.; Rix, A.J. Influences of Energy throughput on the Life of Various Battery Technologies. In Proceedings of the 6th South African Solar Energy Conference, Mpekweni Beach Resort, South Africa, 25–27 November 2019.
26. Aksanli, B.; Rosing, T.; Pettis, E. Distributed battery control for peak power shaving in datacenters. In Proceedings of the 2013 International Green Computing Conference Proceedings, Arlington, VA, USA, 27–29 June 2013. [CrossRef]
27. Ci, S.; Lin, N.; Wu, D. Reconfigurable Battery Techniques and Systems: A Survey. *IEEE Access* **2016**, *4*, 1175–1189. [CrossRef]
28. Dubarry, M.; Baure, G.; Pastor-Fernández, C.; Yu, T.F.; Widanage, W.D.; Marco, J. Battery energy storage system modeling: A combined comprehensive approach. *J. Energy Storage* **2019**, *21*, 172–185. [CrossRef]
29. Varela Barreras, J. Practical Methods in Li-ion Batteries for Simplified Modeling, Battery Electric Vehicle Design, Battery Management System Testing and Balancing System Control. Ph.D. Thesis, Aalborg University, Aalborg, Denmark, 2017.
30. Rehman, M.M.U.; Zhang, F.; Evzelman, M.; Zane, R.; Smith, K.; Maksimovic, D. Advanced cell-level control for extending electric vehicle battery pack lifetime. In Proceedings of the 2016 IEEE Energy Conversion Congress and Exposition (ECCE), Milwaukee, WI, USA, 18–22 September 2016. [CrossRef]
31. Li, Y.; Han, Y. A Module-Integrated Distributed Battery Energy Storage and Management System. *IEEE Trans. Power Electron.* **2016**. [CrossRef]
32. Kim, T.; Qiao, W.; Qu, L. A series-connected self-reconfigurable multicell battery capable of safe and effective charging/discharging and balancing operations. In Proceedings of the 2012 Twenty-Seventh Annual IEEE Applied Power Electronics Conference and Exposition (APEC), Orlando, FL, USA, 5–9 February 2012; pp. 2259–2264. [CrossRef]
33. Frost, D.F.; Howey, D.A. Completely Decentralized Active Balancing Battery Management System. *IEEE Trans. Power Electron.* **2018**, *33*, 729–738. [CrossRef]
34. Liu, C.; Gao, N.; Cai, X.; Li, R. Differentiation Power Control of Modules in Second-life Battery Energy Storage System Based on Cascaded H-bridge Converter. *IEEE Trans. Power Electron.* **2019**. [CrossRef]
35. Araujo, L.S.; Fernandes, N.T.D.; Brandao, D.I.; Cardoso Filho, B.J. SmartBattery: An Active-Battery Solution for Energy Storage System. In Proceedings of the 2019 IEEE 15th Brazilian Power Electronics Conference and 5th IEEE Southern Power Electronics Conference (COBEP/SPEC), Santos, Brazil, 1–4 December 2019.
36. Bouchhima, N.; Gossen, M.; Schulte, S.; Birke, K.P. Lifetime of self-reconfigurable batteries compared with conventional batteries. *J. Energy Storage* **2018**, *15*, 400–407. [CrossRef]

37. Chowdhury, S.; Bin Shaheed, M.N.; Sozer, Y. An integrated state of health (SOH) balancing method for lithium-ion battery cells. In Proceedings of the 2019 IEEE Energy Conversion Congress and Exposition (ECCE), Baltimore, MD, USA, 29 September–3 October 2019; pp. 5759–5763. [CrossRef]
38. De Beer, B. Evaluate and Design Battery Support Services for the Electrical Grid. Master's Thesis, Stellenbosch University, Stellenbosch, South Africa, 2017.
39. Liang, M.; Fu, C.; Xiao, B.; Luo, L.; Wang, Z. A fractal study for the effective electrolyte diffusion through charged porous media. *Int. J. Heat Mass Transf.* **2019**, *137*, 365–371. [CrossRef]
40. Braco, E.; Martin, I.S.; Sanchis, P.; Ursúa, A. Characterization and capacity dispersion of lithiumion second-life batteries from electric vehicles. In Proceedings of the 2019 IEEE International Conference on Environment and Electrical Engineering and 2019 IEEE Industrial and Commercial Power Systems Europe, Genova, Italy, 11–14 June 2019. [CrossRef]
41. Timmermans, J.M.; Nikolian, A.; De Hoog, J.; Gopalakrishnan, R.; Goutam, S.; Omar, N.; Coosemans, T.; Van Mierlo, J.; Warnecke, A.; Sauer, D.U.; et al. Batteries 2020—Lithium-ion battery first and second life ageing, validated battery models, lifetime modelling and ageing assessment of thermal parameters. In Proceedings of the 2016 18th European Conference on Power Electronics and Applications (EPE'16 ECCE Europe), Karlsruhe, Germany, 5–9 September 2016. [CrossRef]
42. Battery: Generic Battery Model Description. Available online: https://www.mathworks.com/help/physmod/sps/powersys/ref/battery.html (accessed on 17 September 2019).
43. Hong, Y.; Wang, S.; Huang, Z. Efficient Energy Consumption Scheduling: Towards Effective Load Leveling. *Energies* **2017**, *10*, 105. [CrossRef]
44. Ferreira, R.V.R.; Silva, S.S.M.; Brandao, D.D.I.; Antunes, H.H.M.; Fernandes, N.T.N. Assessment of energy storage viability for a PV power plant injecting during peak load time. In Proceedings of the 2017 IEEE 8th International Symposium on Power Electronics for Distributed Generation Systems (PEDG), Florianopolis, Brazil, 17–20 April 2017. [CrossRef]
45. Blair, N.; Dobos, A.P.; Freeman, J.; Neises, T.; Wagner, M.; Ferguson, T.; Gilman, P.; Janzou, S. *System Advisor Model, Sam 2014.1. 14: General Description*; Technical Report; National Renewable Energy Lab.(NREL): Golden, CO, USA, 2014.
46. Omar, N.; Monem, M.A.; Firouz, Y.; Salminen, J.; Smekens, J.; Hegazy, O.; Gaulous, H.; Mulder, G.; Van den Bossche, P.; Coosemans, T.; et al. Lithium iron phosphate based battery—Assessment of the aging parameters and development of cycle life model. *Appl. Energy* **2014**, *113*, 1575–1585. [CrossRef]